Dijlah Journal of Medical Sciences (DJMS) Vol. 3, No. 2, May, 2026, pp. 9-27
P-ISSN: 3078-3178, E-ISSN: 3078-8625, paper ID: 02

ORIGINAL ARTICLE

Green Synthesis of Fenugreek-Mediated Silver Nanoparticles with Potent Antioxidant, Antimicrobial, and Selective Cytotoxic Effects against MCF-7 Breast Cancer Cells: Experimental and in Silico Insight

Shahad Basil Ismael*
Department of Molecular and Medical Biotechnology, College of Biotechnology, Al Nahrain University, Baghdad, Iraq

Article Info

Article history:

Received December, 02, 2025
Revised January, 04, 2026
Accepted January, 16, 2026

Keywords:

Fenugreek,
AgNPs ,
Green Synthesis,
Antioxidant Activity,
MCF-7,
MOE

ABSTRACT

Fenugreek (Trigonella *frenum-graecum*), a traditional medicinal herb rich in bioactive phytochemicals, has attracted considerable attention for its antioxidant and anticancer properties. In this study, a green synthesis approach was developed to produce silver nanoparticles (AgNPs) using aqueous fenugreek leaf extract and evaluated their antioxidant, antimicrobial and cytotoxic effects against breast cancer cell (MCF-7). Antioxidant potential was conformed through total phenolic and flavonoid content, reducing power, and DPPH radical scavenging assays, with fenugreek extract showing strong activity compared to standard. The formation of AgNPs was validated by UV-Vis spectroscopy(surface plasmon resonance peak at ~418), fourier-tansform infrared spectroscopy (FTIR) indicating involvement of hydroxyl and carbonyl groups in reduction/capping, and atomic force microscopy(AFM) revealing nanoscale particle size(62-80nm). The green-synthesized AgNPs exhibited significant antibacterial and antifungal activity, with inhibition zones of up to 33 mm against Pseudomonas aeruginosa and 42mm against Candida albicans. Cytotoxicity assays on MCF-7 cells demonstrated dose-dependent effects, with an IC_{50} of 112.4µg/mL while normal fibroblasts (HdFn) remained comparatively less affected (IC_{50}= 140.4), suggesting selective toxicity. To complement these findings, molecular docking was performed for three major fenugreek phytochemicals-diosgenin, quercetin, and trigonelline against breast cancer relevant proteins (*ERα* , *EGFR*, and *BCL-2*). Diosgenin and quercetin exhibited strong binding affinities (-8.6 to -9.2 kcal/mol), indicating potential apoptotic and antiproliferative mechanisms underlying the observed cytotoxicity. Together, the results highlights *foenum-graecum* mediated AgNPs as a promising biogenic nanoplatform with potent antioxidant, antimicrobial, and anticancer activities, warranting further in vivo validation for breast cancer therapy.

Corresponding Author:

* Shahad Basil Ismael
Department of Molecular and Medical Biotechnology, College of Biotechnology, Al-Nahrain University, Baghdad, Iraq
Email: **shahad.basil@nahrainuniv.edu.iq**

1- INTRODUCTION

Trigonella frenum-graecum(fenugreek), a leguminous plant of the Fabaceae family, has gained significant attention because of its nutritional and medicinal properties[1]. Various plant parts- leaves, seeds, and roots- are rich in diverse phytochemicals, including alkaloids, flavonoids, saponins, and phenolic compounds, many of which possess antioxidant, anti-inflammatory, and anticancer properties [2]. Nanotechnology has emerged as a rapidly expanding field in biomedical research, offering innovative solutions for drug delivery, diagnostics, and therapeutic intervention[3]. However, conventional chemical synthesis methods often involve toxic reducing agents, limiting their biomedical applicability. To overcome these limitations, green synthesis methods using plant extracts have been proposed as simple, cost effective, and environmentally safe alternatives[4] .Despite these advances , few studies have explored the use of fenugreek leaf extract in nanoparticle synthesis , particularly in the context of breast cancer therapy. The MCF-7 cell line, a widely studied estrogen receptor positive breast cancer model, provides a robust system for evaluating the anticancer activity of novel nanomaterials. In present study reported the green synthesis of silver nanoparticles using aqueous fenugreek leaf extract [5].

This study aims to evaluate antioxidant potential of the aqueous extract of fenugreek, antimicrobial, and cytotoxic activities of green- synthesized silver nanoparticles (AgNPs)Furthermore, to complement the in vitro data, performed in silico molecular docking of major feungreek phytochemicals (diosgenin, quercetin, and trigonelline) against key breast cancer associated proteins(*ERα* , *EGFR* , and *BCL-2*). The integrative approach highlights the potential of fenugreek functionalized AgNPs as abiogenic nanoplatform for breast cancer therapy.

2- MATERIALS AND METHODS

2.1 Plant collection and identification

Trigonella foenum-graecum (Fenugreek) was supplied from Al-Razi Center for Medical Herbes between October and November of 2024, as previously authorized by the Iraqi national herbarium. Plant leaves were cleaned to get rid of dust and other debris. The dried leaves were pulverized into a fine powder using a Wiley Mill grinder (Standard Model No. 3) and then sterilely stored until the next experiment.

2.2 Aqueous extraction of *Trigonella foenum-graecum* (Fenugreek)

Fenugreek aqueous extract was prepared according to previously described method [6].

2.3 Determination of the active phytochemicals in Fenugreek plant

Determination of the active phytochemicals in Fenugreek plant was achieved in Biotechnology research center in AL-Nahrain University.

2.3.1 Estimation of total flavonoid, phenolic content and saponin

Total flavonoid content was determined using spectrophotometric aluminum chloride colorimetric assay with rutin as the reference standard[7]. The absorbance was measured at 450 nm, and quantification was based on a rutin calibration curve (2.5-80 µg\mL).Total phenolic content (TPC) estimated using Folin-Ciocalteu method with gallic acid as standard, and absorbance was estimated at 527 nm. Results were expressed as mg gallic acid equivalents per100 g of dry sample[8].total saponin content was quantified spectrophotometrically using an acetic acid- sulfuric reagent with leanolic acid as the references standard (0-100 µg\mL), and absorbance was measured at 527 nm Results were expressed as grams of Oleanolic acid equivalents per100 g of dry sample [9].

2.4 Assessment of antioxidant activity (in vitro)

The antioxidant potential of the aqueous extract of Trigonella *frenum graecum* (feungreek) was assessed using two complementary assays [10].

2.4.1 DPPH Radical Scavenging Activity:

The method was used to evaluate the antioxidant activity of the aqueous extract of fenugreek and standard (vitamin C),.The absorbance of each solution was measured using a spectrophotometer at 517 nm, and the result can be calculated using the equation that follows[11]:

$$\text{DPPH radical scavenging activity (\%)} = \left(1 - \frac{\text{Absorbance of Sample}}{\text{Absorbance of Standard}}\right) \times 100$$

2.4.2 Ferric reducing antioxidant power (FRAP) assay

The reductive potential the fenugreek aqueous extract was evaluated following the method of [12], The absorbance of the final mixture was recorded at 700 nm. Trolox solution prepared under the same conditions was used as the standard. All measurement were performed triplicate, and results were expressed as mean ±SD [13].

2.5 Biosynthesis of sliver nanoparticle:

Green synthesized nanoparticles were prepared by adding 9 ml of various $AgNO_3$ concentrations (1.0, 1.5, 2, and 2.5 mM) flowed 1 ml of aqueous extract. The mixtures were incubated at 30°C in the dark to prevent photoactivation of silver nitrate under static conditions [14].

2.6 Characterization of synthesized silver nanoparticles:

Green synthesized silver nanoparticles were characterized by color changing after 2 and 24 hr which considered as an important method for early detection of synthetic green NPs [15]. ***Ul***traviolet-Visible Spectrophotometer (UV-VIS) was conducted by employing a UV-visible spectrophotometer (Shimadzu,UV- 1800, Japan) at room temperature in range of 200-800 nm to determine the optical properties [16].The FT-IR spectra (Model 8400S Shimadzu spectrophotometer, Japan) in the frequency range 4000-400 cm^{-1} were recorded to characterize the absorption bands[17]. Atomic Force Microscopy (AFM, model AA3000, Angstrom Advanced Inc., USA), the slide was placed on the AFM sample stage, and analysis was performed in accordance with standard protocol [18].

2.7 Antimicrobial potentials of green synthesized sliver nanoparticle

The assay of antimicrobial activity includes estimation of both antibacterial and antifungal affected of green synthesized sliver nanoparticles (AgNPs) loaded on Fenugreek against three G- and one p G+ bacteria in-addition to *Candida albicans*(fungi) [19].

2.7.1 Preparation Media

Muller-Hinton agar was formerly prepared by dissolving 38g/l distilled water, adjusting pH to 6.8,and autoclaving at 121°C. Following solidification, plates were maintained at 4°C and lastly stuffed with 30 µL of green-synthesized nanoparticles pathogenic microorganism used include S*taphylococcus aureus; Pseudomonas aeruginosa; Escherichia coli*; *Enterobacter* and *Candida albicans*) inoculum turbidity was adjusted to 0.5 McFarland standard 1.5 x 10^8 cells/ml,[20] . wells were made in the agar and fill with different concertation(1-2.5mM) of AgNPs , The plates were incubated at 37^oC for 18 to 24 hours. After incubation, the zones of inhibition were measured in millimeter.

2.8 Cytotoxic activity of fenugreek mediated silver nanoparticles ion MCF-6 cells (MTT Assay)

Green synthesized nanoparticles were examined for their cytotoxic effect against human breast cancer cell line MCF-7 using the MTT colorimetric assay (Bio-Rad, USA)based on preliminary findings (AgNPs) synthesized at a concentration 2mM were selected for further testing ,serial dilution of AgNPs (12.5-400 ug/ml) were prepared ,MCF-7 cells, briefly were washed with PBS, detached using trypsin- versine and resuspend in RPMI media ,cell density was adjusted using hemocytometer , and a 1×10^4 to1×10^6were grown in 96 -well microtiter plates at a final volume of 200 per well at 37 °C, 5% CO_2 for 24h after incubation the cells were treated with Serial dilutions of desired compound 24h under the same condition [21], Subsequently, 10 µlof MTT reagent was added to each well and incubated for 4h.The media was carefully removed, and 100 µl of solubilization solution was added into each well and incubated 5 min. Formazan formation was determined by measuring the absorbance at 570 nm using an ELISA microplate reader.

2.9 Statistical Analysis

The parameters under investigation were expressed as mean ± standard deviation (SD), and the program SPSS version 13.0 was used to perform an analysis of variance (ANOVA) to evaluate mean differences. In cases where the probability value (p) was equal to or less than 0.05, the difference was deemed significant.

2.10 Bioinformatics and Molecular Docking Analysis

2.10.1 Selection of Major Bioactive Compounds in Fenugreek

A literature review and database search (PubChem, ChEMBL) were conducted to identify predominant phytochemicals in Trigonella foenum-graecum [22]. The three most cited bioactive compounds with potential anticancer effects were selected: diosgenin, trigonelline, and quercetin. The 3D structures of these molecules were retrieved in SDF format from the PubChem database and converted to PDBQT format using Open Babel for docking studies.

2.10.2 Target Protein Selection and Preparation

To ensure reliable docking simulations, three human protein targets with well-established roles in breast cancer progression were selected : Estrogen Receptor alpha (*ERα* with PDB ID: 3ERT), Epidermal growth Factor Receptor (*EGFR* with PDB ID: 1M17) and B-cell lymphoma 2 (*BCL-2* with PDB ID: 1GJH). The crystal structures of these proteins were retrieved from the protein data bank(PDB) in pdb format [23].

2.10.3 Molecular Docking Protocol

Docking simulations were performed using AutoDock Vina within the PyRx environment. Each ligand was docked against the selected proteins using default grid box parameters centered on the active site. The binding affinity (ΔG in kcal/mol) of each ligand to each protein was recorded,. Docking poses with the lowest binding energies were visualized and analyzed using Discovery Studio Visualizer to examine hydrogen bonds and hydrophobic interactions [24].

3- RESULTS AND DISCUSSION

3.1 Detection of active constituents in Fenugreek

Fenugreek contained the following active constituent tannins, polysaccharide, alkaloids, saponins, flavonoids and polyphenols as shown in Table 1.

Table (1): Major active constituent in Fenugreek aqueous extract

Chemical compounds	Reagents	Indication	Results
Tannins	Ferric chloride	Red-ppt	Positive
Polysaccharide	Fehling reagent	Red-ppt	Positive
Flavonoids	Ammonia	Red-ppt	Positive
Saponins	1-shaking of extract 2-Mercuric chloride	Foam White -ppt	Positive
Alkaloids	Myers reagent	White -ppt	Positive
Polyphenols	3%ferric chloride	Green-blue ppt	Positive

3.2 Determination total Flavonoids, phenolic and saponin

Aqueous extract of Fenugreek exhibited a total flavonoids content of 469.4 ± 3.267 µg/ml,While total phenolic were 182.1 ± 0.449 µg/ml and total saponins were 145.2± 2.160 µg/ml in Table 2.

Table (2): Total flavonoid, phenol and saponin contents of fenugreek

Total Fenugreek active constituents	Mean. ± SD
Total flavonoid	469.4 ± 3.267
Total phenol	182.1 ± 0.449
Total saponin	145.2± 2.160

3.3 In *vitro* Determination of antioxidant activity of aqueous extract of Fenugreek

Fenugreek aqueous exhibited strong antioxidant activity in FRAP assay and DPPH assays, showing a concentration-depended increase in reducing power and significantly higher radical scavenging activity compered to Trolox and vitamin C at all tested concentration as as shown in Table 3,Table 4.

Table (3): Reductive ability of aqueous extract of Fenugreek and trolox (vitamin E)

Concentration	Reductive Ability (Mean ± SD)	
(mg/ml)	***Trigonella foenum graecum* aqueous extract**	**Trolox (Vitamin E)**
0.08	0.77± 0.16	0.108 ± 0.001
0.16	0.89 ± 0.01	0.114 ± 0.004
0.32	0.92 ± 0.25	0.132 ± 0.007
0.64	0.96 ± 0. 19	0.211 ± 0.015

Table (4): DPPH radical scavenging activity of aqueous extract of Fenugreek and vitamin C

Concentration (mg/ml)	DPPH Radical Scavenging Activity (Mean ± SD; %)	
	Aqueous extract of Fenugreek	Vitamin C
0.062	75.23 ± 12.17	39.66 ± 2.52
0.125	79.33 ±13.09	41.33 ± 10.01
0.25	81.22 ± 15.01	48.33 ± 8.50
0.5	89.24 ±12.57	53.00 ± 10.53

3.4 Synthesis and Characterization of silver nanoparticles (Ag NPs)

The first evidence of a synthesis reaction, the color of silver colloidal solutions changes from colorless to yellow color, it was noticed as (Fig.1 A and B).These changes indicate the formation of silver nanoparticles and are caused by the reduction of silver metal ions Ag into silver nanoparticles.

.

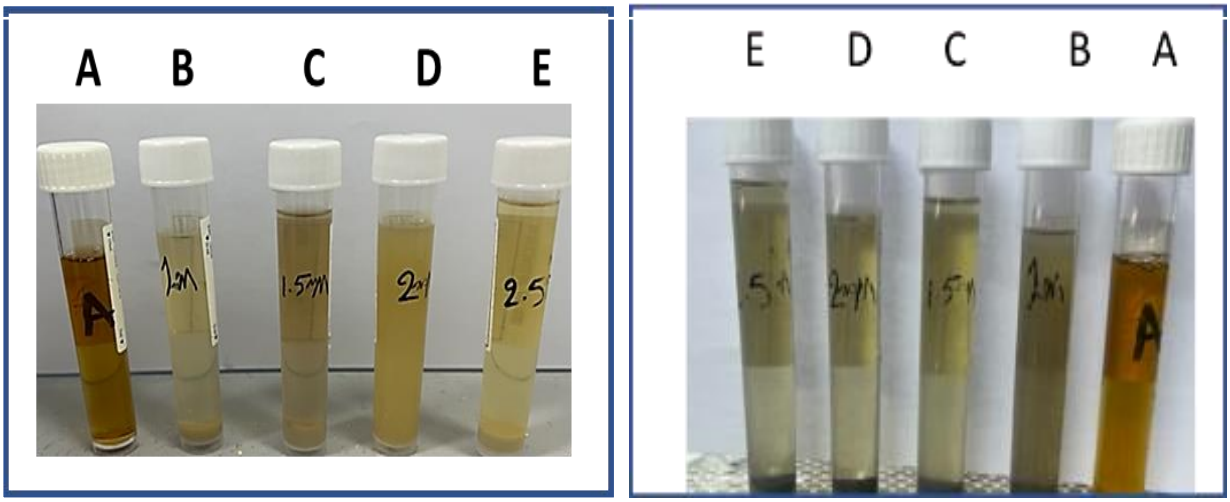

Fig (1): Visual observation of green synthesized

nanoparticle (A)After2hr where: (B)(C(D)(E) fenugreek extract loaded with nanoparticle with different Ag molarity (1,1.5,2 and sliver2.5 mM). while (A) represent fenugreek aqueous extract without AgNo3 and (B) After24hr where: (B)(C(D)(E) fenugreek extract loaded with sliver nanoparticle with different Ag molarity (1,1.5,2 and 2.5 mM). while (A) represent fenugreek aqueous extract without AgNo3

UV-Visible spectroscopy enables the investigation of the production and stabilization of AgNPs. The surface resonance plasmon (SPR) band of biosynthesized AgNPs was identified at around 418 nm, as illustrated in Fig.2. The dimensions, form, morphology, dielectric constant of the medium, and the chemical environment of produced nanoparticles influence the absorption spectra of AgNPs. The results align with prior observations of biogenic Ag-NPs generated using different plants. The energy band gap of Ag-NPs generated from fenugreek leaf extract and the absorbance peak observed in the UV-Vis spectrometer at different time intervals, with a peak at 420 nm corresponding to Ag-NPs absorbance. Finally, the characteristic surface plasmon resonance (SPR) absorption band is considered as evidence of the reduction of silver ions (Ag^{+}) to metallic silver (Ag^{0}), which confirms the success of the biosynthesis process of silver nanoparticles.

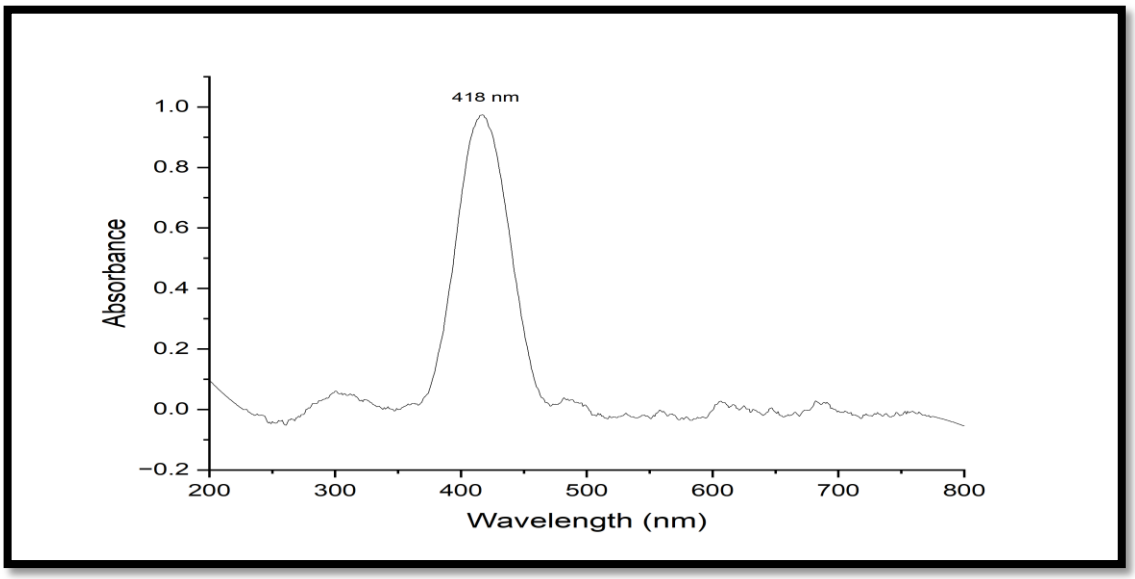

Fig (2): UV-visible absorption sepectrum of feungreek-mediated silver nanoparticles showing a distinct surface plasmon resonance (SPR) peak at 418, confirming successful NPs synthesis

According to FTIR analysis was employed to identify the various functional groups present in the leaf extract and on the surface of the biosynthesized AgNPs. The functional groups were chiefly accountable for the formation of silver nanoparticles by the reduction of silver ions Ag^{+} into silver nanoparticles Ag and the stabilization of the biosynthesized AgNPs. As shown in Figure 3 (red line), the FTIR spectrum analysis of the aqueous leaf extract indicates the presence of distinct peaks at 3253.15, 2933.07, 1590.82, 1398.08, 1057.39,843,775,613, and 530 cm^{-1}. The synthesized of AgNPs exhibited peaks at 3239.38, 2912.42, and 1394.46 cm^{-1}, were associated with stretching vibrating of hydroxyl groups (O-H) and alkane (C-H). The peaks at 1580.49 and 764,599 cm^{-1} are according to the bending vibrating of alkene (C=O) groups. The band at 1036.7 cm^{-1} was related to the amide band containing carbonyl groups (C=O). The peak at 513.57 cm-1 is attributed to Ag-O bond, confirming successful synthesis of Ag NPs as illustrated in, **Fig.3.** The FTIR spectrum confirms that phenolic, carbonyl and alcohol groups in the fenugreek extract played a significant role in reducing Ag+ to Ag NPs a stabilizing agent. The emergence of new peaks in the 500-600 cm^{-1} range confirms formation of Ag-O bonds, characteristic of Ag NPs.

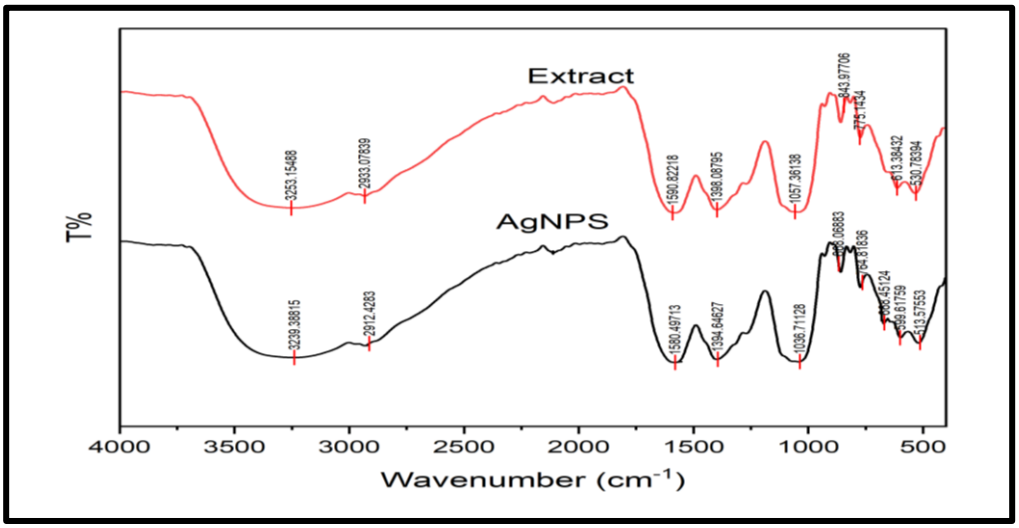

Fig (3): Comparative FTIR profiles of feungreek extract (red) and AgNPs (black), which indicating key functional group and Ag-O bond formation

Other hand, atomic force microscope (AFM) images as Fig.4. The average particle size of fenugreek loaded with sliver nanoparticles at 1 mM of green synthetic NPs with an average size of 62 nm was determined using an atomic force microscope (AFM). In contrast, the average size of green synthetic NPs at 1.5 mM was 70 nm, while the average size at 2 mM was the size 66 nm, and the average size at 2.5 mM was the size 80 nm.

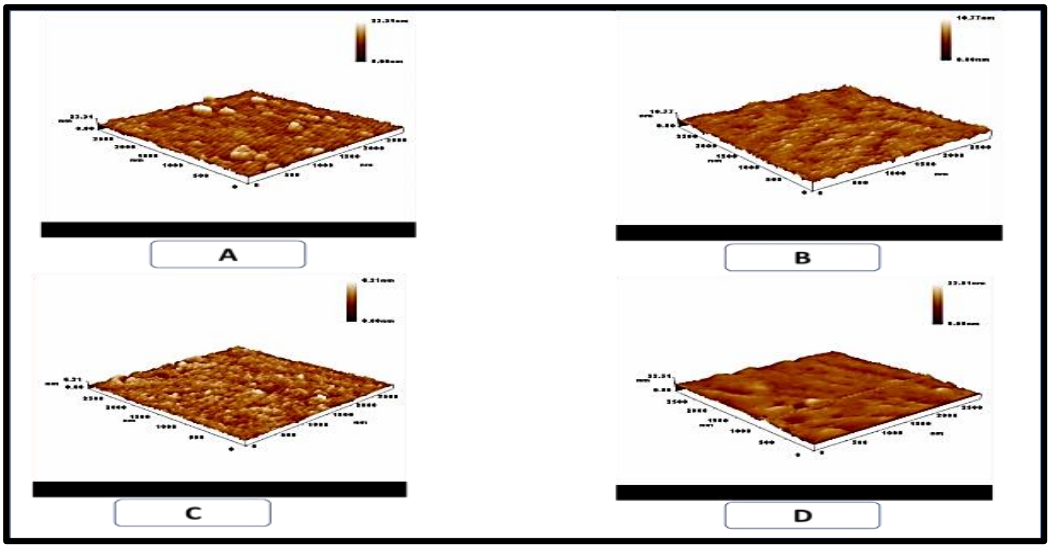

Fig (4): Atomic force microscopy (AFM) surface morphologies of feungreek -mediated silver nanoparticles synthesis at differentational precursor concentration. A.1mM AgNPs with an average particle size of 62nm; B.1.5mM AgNPs with an average particle size of 70nm; C.2mM AgNPs with an average particle size of 66nm; D. 2.5 mM AgNPs with an average particle size of 80nm; The images demonstrate concentration-dependant variations in nanoparticles size and surface roughness

3.5 Antimicrobial potential for green synthesized sliver nanoparticle loaded on Fenugreek

Aqueous extract of Fenugreek and green biosynthesized AgNPs of different molarity showed a variety zone of inhibition as showed in Table 5 , the inhibition zone for 1Mm ranged from 33,22,14 ,20 and 36 mm for *Pseudomonas Aeruginosa, Staphylococcus Aureus, E.col ,Enterobacter and Candida albicans r*espectively , while inhibition zone for 1.5Mm ranged from 30,20,11,22 and 35mm for *Pseudomonas Aeruginosa, Staphylococcus Aureus, E.col ,Enterobacter and Candida albicans* respectively , while inhibition zone for 2Mm ranged from 30,25,15,21and ,40mm for *Pseudomonas Aeruginosa, Staphylococcus Aureus, E.col, Enterobacter and Candida albicans* respectively , while inhibition zone for 2.5Mm ranged from 29,22,16,22 and42 mm for *Pseudomonas Aeruginosa, Staphylococcus Aureus, E.col, Enterobacter and Candida albicans* respectively.

Table 5: Zone of Inhibition (in millimeter) of aqueous extract of fenugreek, silver nanoparticles against clinical and phytopathogenic bacteria

Name of the test Organism	**Zone Of Inhibition (Mm) Of Various Sample**				
	aqueous extract fenugreek	**Green synthesized nanoparticles at different molarity**			
		1Mm	1.5 Mm	2 Mm	2.5 Mm
Pseudomonas Aeruginosa	-	33	30	30	29
Staphylococcus Aureus	-	22	20	25	22
E.col	-	14	11	15	16
Enterobacter	-	20	22	21	22
Candida albicans	-	36	35	40	42

‘-‘ no activity

After testing aqueous extracts of Fenugreek, it's concluded that no potential of antimicrobial effect, as shown in Fig 5.

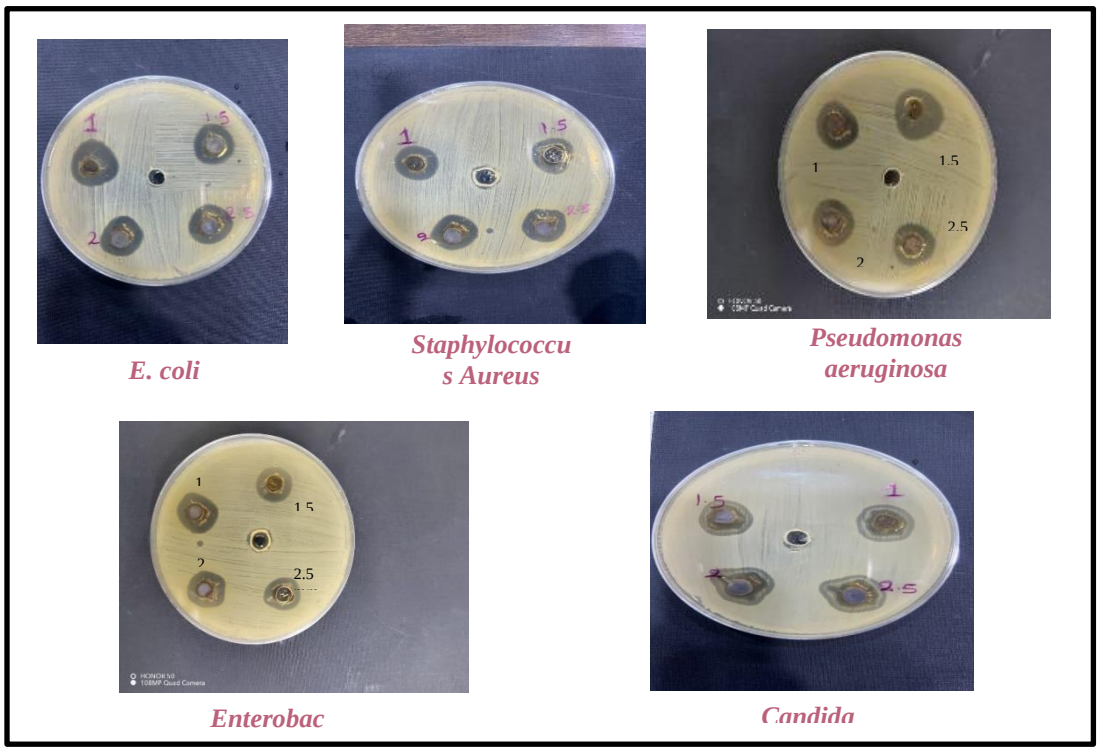

Fig (5): Antimicrobial activity of the AgNPs synthesized using the leave extract of *Trigonella foenum-graecum* L. against some pathogenic microorganism

3.6 Cytotoxic effect of green synthesis nano particles loaded on Fenugreek

MTT experiments (Table 6, Fig. 6) revealed that the growth inhibition of MCF-7 cell after treatment with F-AgNPs was found, The viability of the cells was decreased. At 400µg/ml, the percentage of (MCF-7) cell viability decreased and reached (42.01 ± 2.4 %). At 12.5 µg/ml, the maximum cell viability (MCF-7) was observed, reaching 95.37±1.8%. Green artificial nanoparticles were loaded onto fenugreek and showed the strongest cytotoxic effect, with an IC50 value of 112.4µg/ml.However an IC_{50} of 140.4 µg/ml was obtained from the effect of green synthesized nano particles loaded on Fenugreek on HdFn normal cell line within cell viability ranged from (94.9 ± 2.19 to 70.91 ± 1.2) for 12.5 to 400 µg/ml respectively.

Table (6) : Cytotoxicity effect of green synthesized nano particles loaded on MCF-7 and HdFn cells after 24 hours incubation at 37ºC at 2mµ

Green synthesized nano particles Concentration µg mL^{-1}	Mean viability (%) ± SD	
	HdFn normal cell line	MCF-7 breast cancer cell line
400	**70.91±1.2**	**42.01±2.4**
200	74.46±0.8	50.38±4.84
100	92.12±1.5	71.75±4.11
50	96.18±1.2	88.078±3.2
25	96.95±1.14	94.59±2.16
12.5	94.9±2.19	95.37±1.8

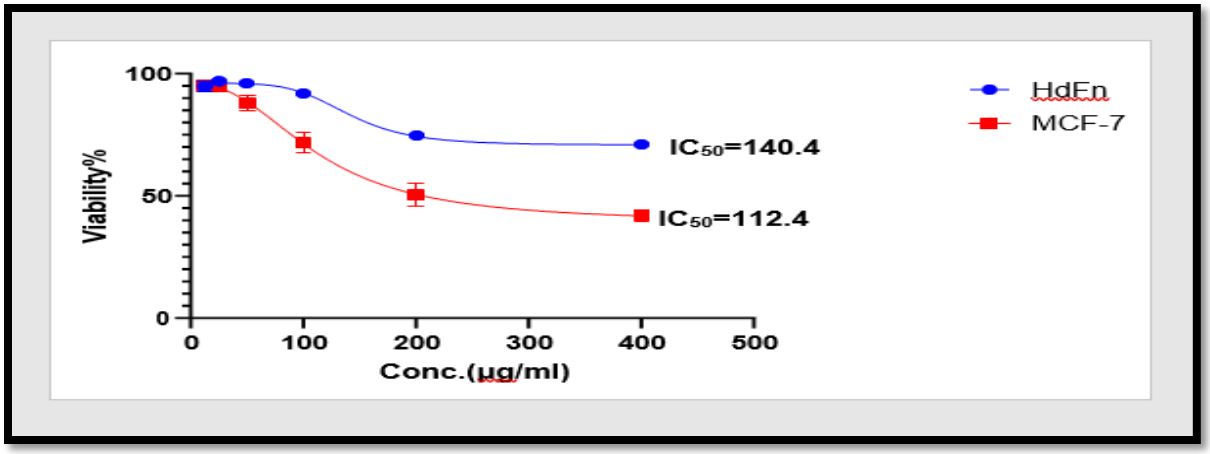

Fig (6): Dose-dependent cytotoxic effect of feungreek-mediated silver nanoparticles on MCF-7 breast cancer cells compared to normal fibroblasts (HdFn), showing IC_{50} value of 112.4µg/ml and 140.4µg/ml , respectively

3.10. Bioinformatics Results

3.10.1 Selection of Major Bioactive Compounds in Fenugreek

Three key bioactive compounds were successfully identified through a combined literature review and cheminformatics database screening (PubChem and ChEMBL)[50]: diosgenin, trigonelline, and quercetin, Fig.7

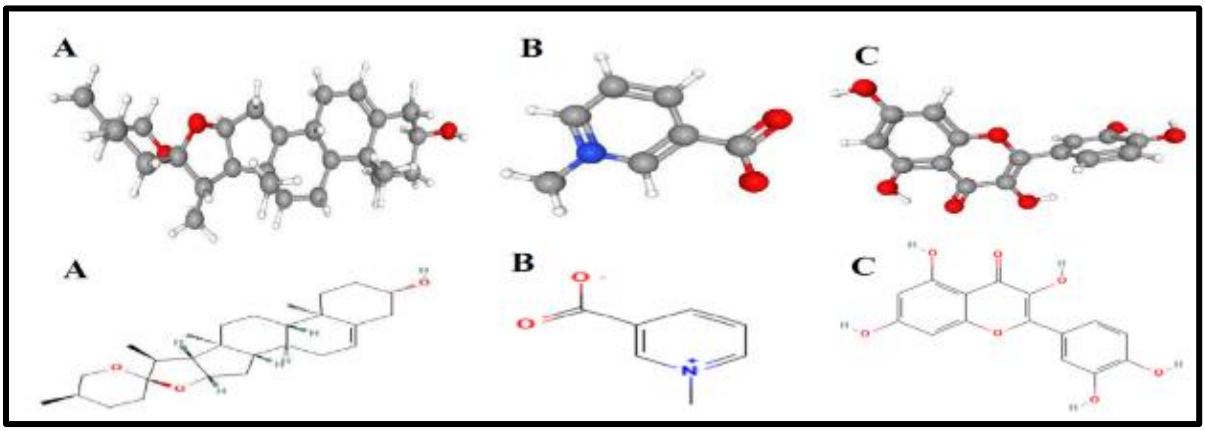

Fig (7): Display the 2D and 3D structure of the three most cited bioactive compounds with potential anticancer effects of Trigonella foenum-graecum, (A)3D and 2D structure of diosgenin, (B) 3D and 2D structure of trigonelline, and (C) 3D and 2D structure quercetin

These phytochemicals were selected based on their documented anticancer, antioxidant, and apoptotic activities, particularly in relation to breast cancer models. The 3D molecular structures of all three compounds were retrieved in Structure Data File (SDF) format from the PubChem database [25]. Each compound was then structurally optimized and converted to PDBQT format using Open Babel, ensuring compatibility with downstream molecular docking platforms such as AutoDock Vina.

This curated panel of compounds served as the ligand dataset for subsequent in silico docking experiments targeting breast cancer-associated proteins[26] ,aiming to investigate the potential molecular interactions underlying the observed cytotoxic effects of fenugreek-loaded silver nanoparticles on MCF-7 cell lines.

3.10.2 Molecular Targets in Breast Cancer

To explore the molecular basis of the cytotoxic activity observed in fenugreek-loaded silver nanoparticles, three key human protein targets associated with breast cancer progression and survival were selected for molecular docking analysis which includes ;Estrogen Receptor alpha (*Erα* , PDB ID: 3ERT) , Epidermal Growth Factor Receptor (*EGFR*, PDB ID: 1M17), and B-cell lymphoma 2 (*Bcl-2*, PDB ID: 1GJH) .These targets were chosen based on their

established roles in hormone receptor signaling, cellular proliferation, and anti-apoptotic mechanisms within MCF-7 breast cancer cells. The crystal structures of the selected proteins were retrieved from the Protein Data Bank (PDB) and prepared using AutoDock Tools, Fig. 8

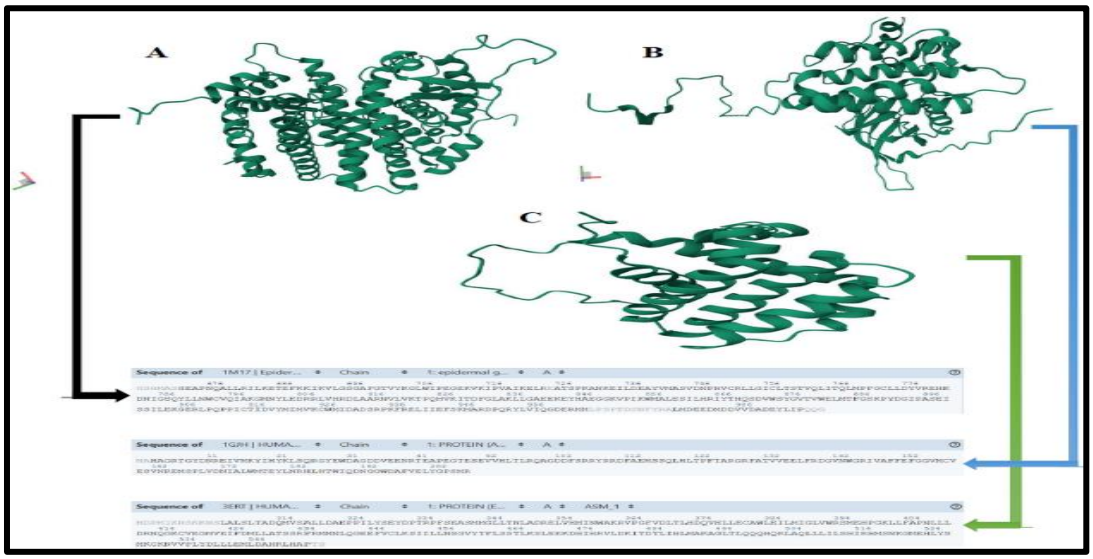

Fig (8): Display the 3D structure of three key human protein targets associated with breast cancer ,(A) Estrogen Receptor alpha (*Erα*, PDB ID: 3ERT) , (B)Epidermal Growth Factor Receptor (*EGFR*, PDB ID: 1M17), and (C) B-cell lymphoma 2 (*Bcl-2*, PDB ID: 1GJH)

Preprocessing included the removal of crystallographic water molecules, addition of polar hydrogen atoms, and assignment of Koll man partial charges[27] , to ensure accurate simulation of ligand–receptor interactions. These prepared protein structures were then converted into PDBQT format, ready for docking simulations with the selected fenugreek phytochemicals. This step ensured the structural and electrostatic compatibility of the receptor models for high-accuracy binding affinity predictions.

3.10.3: Binding Affinities

Molecular docking simulations revealed that all three fenugreek-derived compounds diosgenin, quercetin, and trigonelline—demonstrated binding affinity toward key breast cancer-related proteins: (Estrogen Receptor alpha; PDB ID: 3ERT), (Epidermal Growth Factor Receptor; PDB ID: 1M17), and (B-cell lymphoma 2; PDB ID: 1GJH), Fig. (9 to 17).

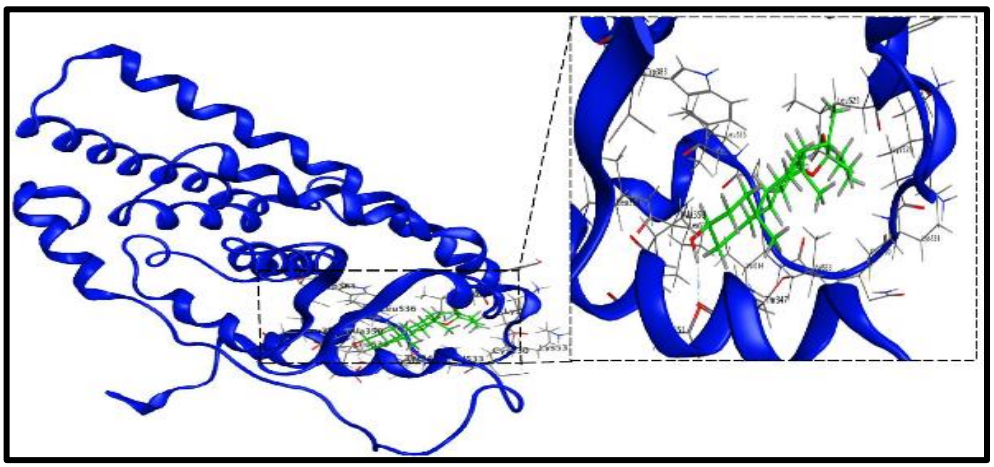

Fig (9): The docking interaction analysis of the top pose between Estrogen Receptor alpha (*ERα*, PDB ID: 3ERT) and Diosgenin

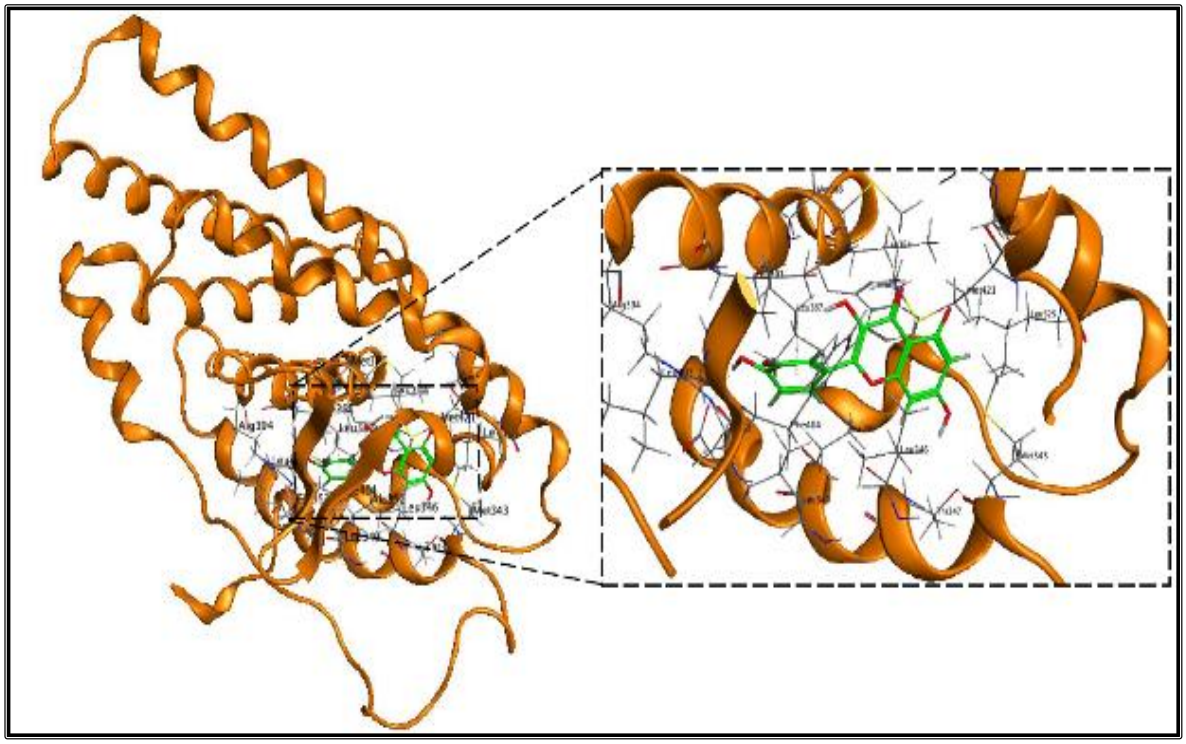

Fig (10): The docking interaction analysis of the top pose between Estrogen Receptor alpha (*ERα*, PDB ID: 3ERT) and Quercetin

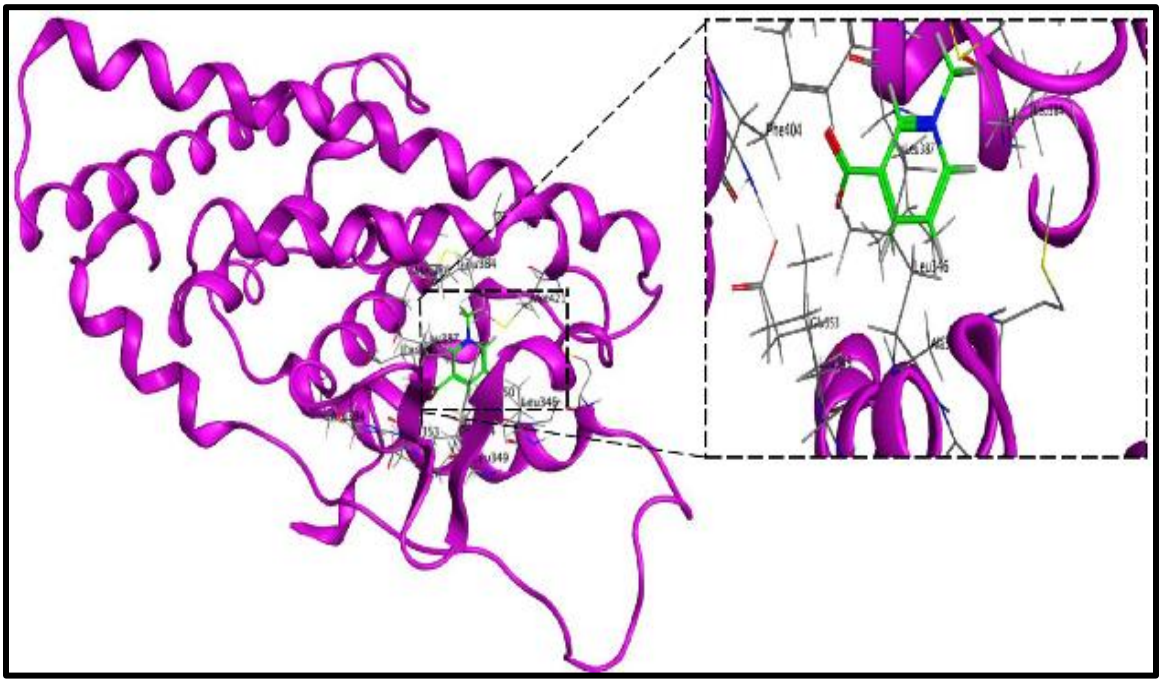

Fig (11): The docking interaction analysis of the top pose between Estrogen Receptor alpha (*ERα*, PDB ID: 3ERT) and Trigonelline

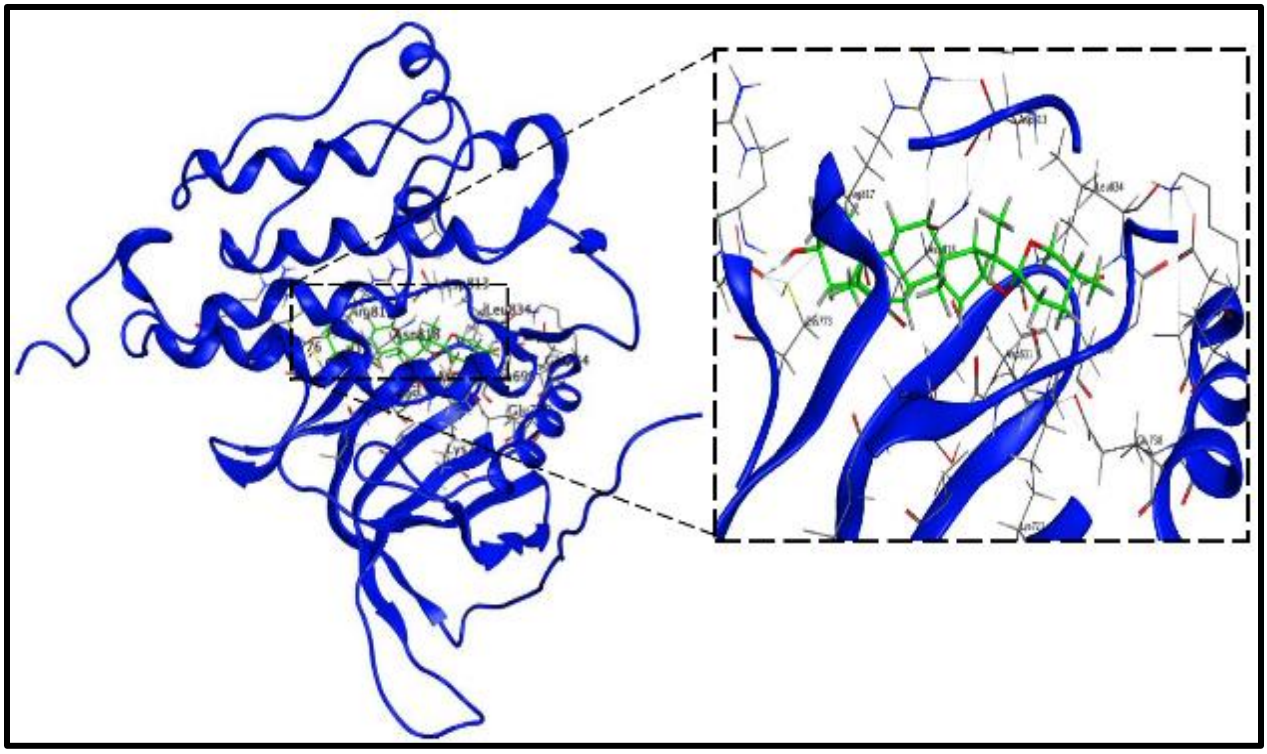

Fig (12): The docking interaction analysis of the top pose between Epidermal Growth Factor Receptor (*EGFR*, PDB ID: 1M17) and diosgenin

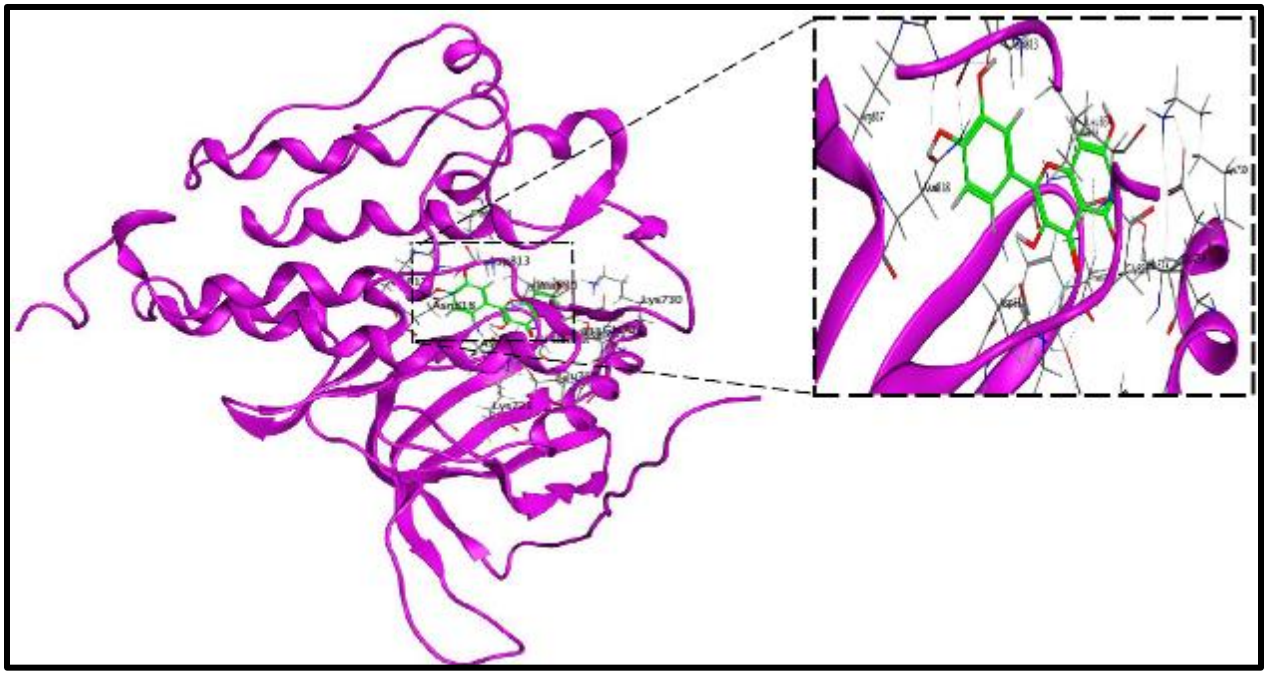

Fig (13): The docking interaction analysis of the top pose between Epidermal Growth Factor Receptor (*EGFR*, PDB ID: 1M17) and Quercetin

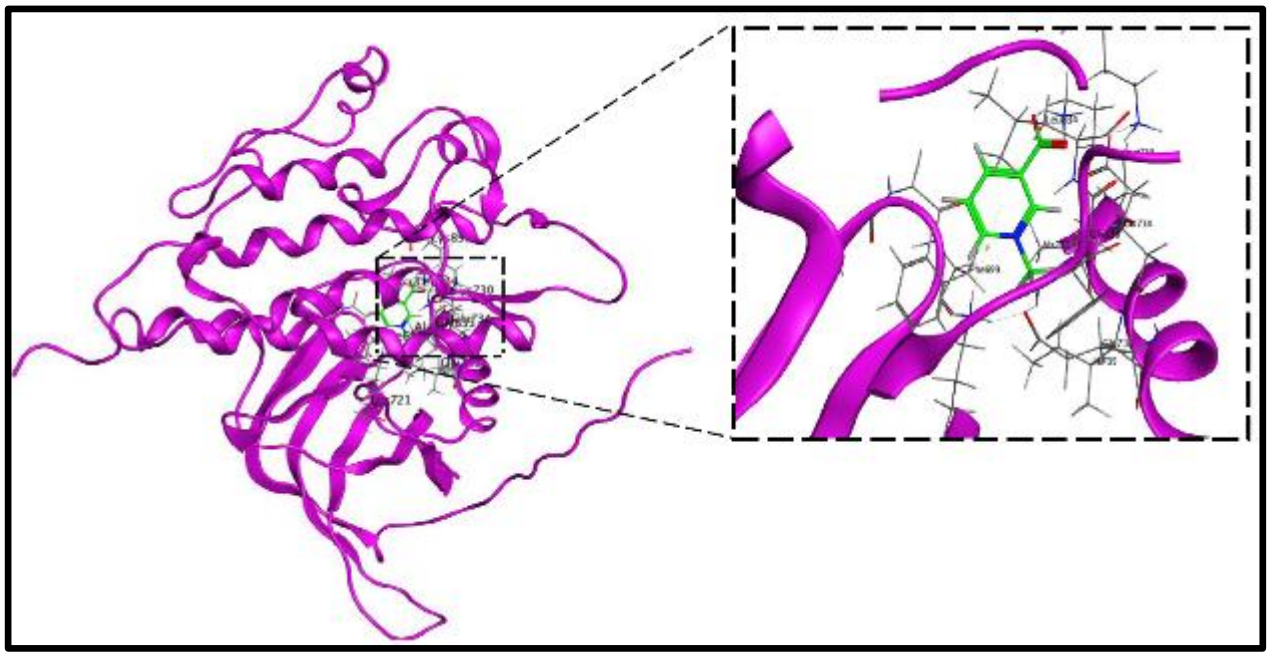

Fig (14): The docking interaction analysis of the top pose between Epidermal Growth Factor Receptor (*EGFR*, PDB ID: 1M17) and Trigonelline

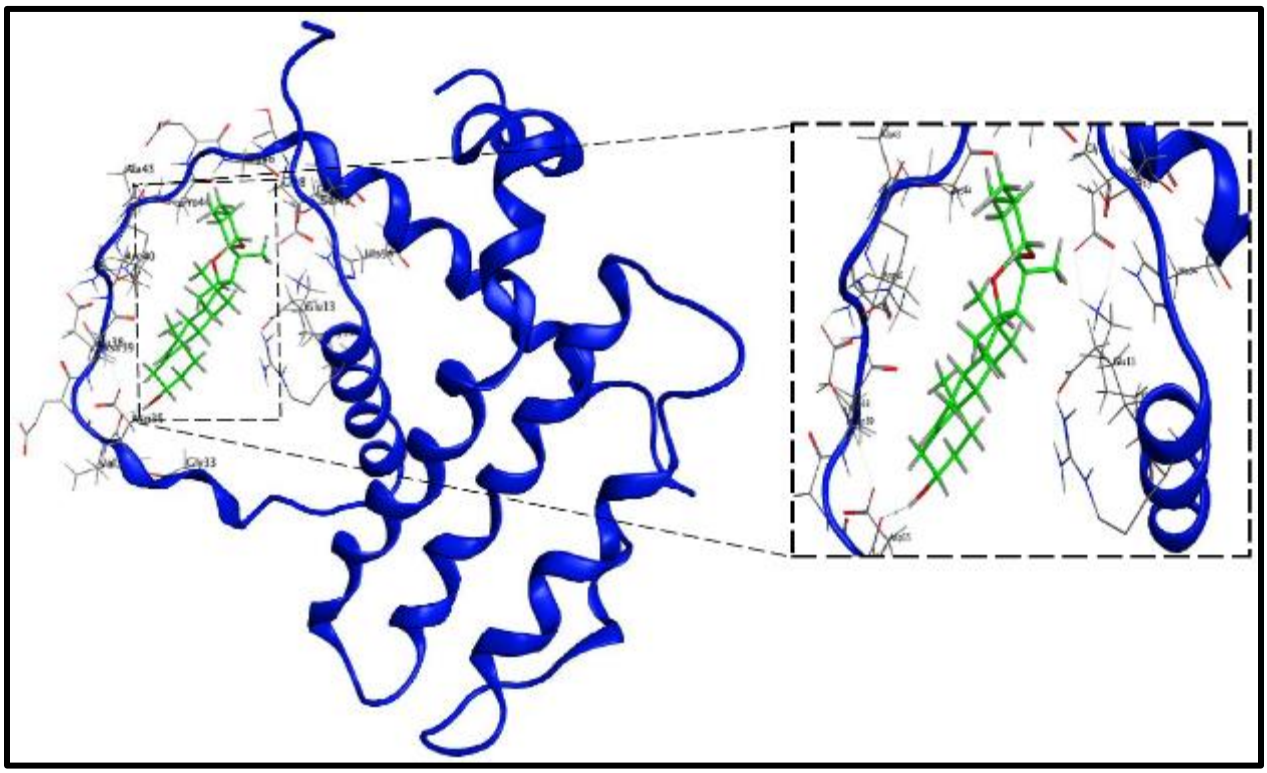

Fig (15): The docking interaction analysis of the top pose between B-cell lymphoma 2 (*Bcl-2*, PDB ID: 1GJH) and diosgenin

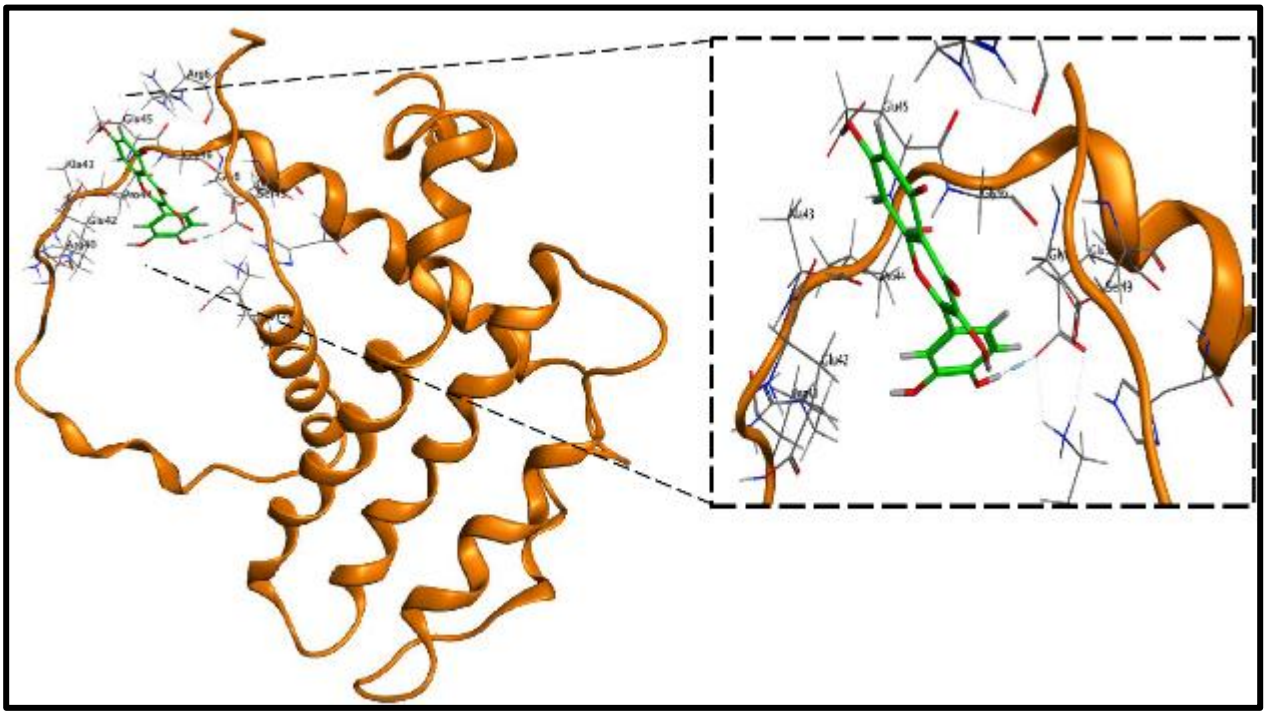

Fig (16): The docking interaction analysis of the top pose between B-cell lymphoma 2 (*Bcl-2*, PDB ID: 1GJH) and Quercetin

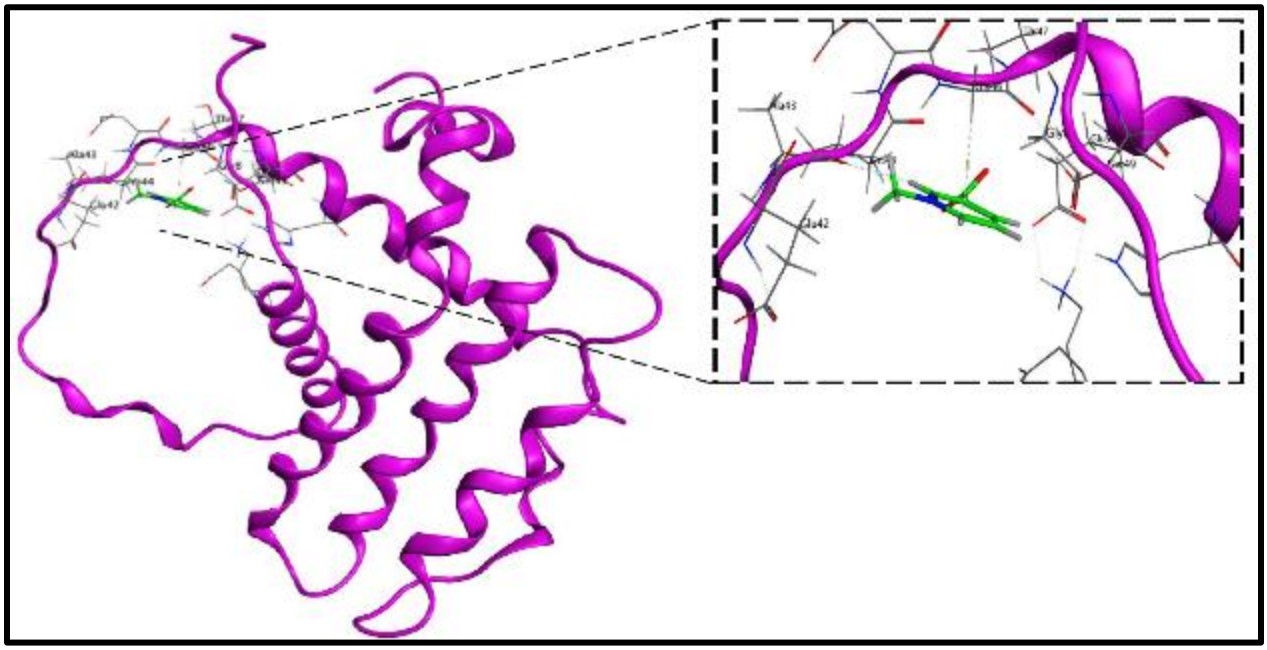

Fig (17): The docking interaction analysis of the top pose between B-cell lymphoma 2 (*Bcl-2*, PDB ID: 1GJH) and Trigonelline

As summarized in the table below, diosgenin exhibited the strongest binding, particularly to *ERα* (–9.2 kcal/mol) and Bcl-2 (–8.9 kcal/mol), while quercetin showed consistently high affinities, with the lowest binding energy recorded for *Bcl-2* (–9.1 kcal/mol). In contrast, trigonelline displayed comparatively weaker interactions, with binding energies around –6.5 to –6.7 kcal/mol. Notably, both diosgenin and quercetin surpassed the –8 kcal/mol threshold, indicating high-affinity binding, especially toward proteins involved in apoptosis and proliferation pathways such as *Bcl-2* and *EGFR*. These findings support the potential therapeutic relevance of these phytochemicals and warrant further investigation through in vitro and in vivo models, (table 7 and 6).

Table (7): The three fenugreek-derived compounds showed notable binding to breast cancer-related proteins

Compound	*ERα* (3ERT)	*EGFR* (1M17)	*Bcl-2* (1GJH)
Diosgenin	–9.2 kcal/mol	–8.6 kcal/mol	–8.9 kcal/mol
Quercetin	–8.7 kcal/mol	–9.0 kcal/mol	–9.1 kcal/mol
Trigonelline	–6.4 kcal/mol	–6.7 kcal/mol	–6.5 kcal/mol

Table (8): Molecular Docking Results of Diosgenin, Quercetin and Trigonelline Complexes with 3ERT, 1M17 and 1GJH human protein

Protein–Ligand Complex	Ligand Atom(s)	Receptor Atom(s)	Residue (Chain)	Interaction Type	Distance (Å)
3ERT – Diosgenin	OD1	O3	ASP 351 (A)	H-donor	2.88
3ERT – Quercetin	OE2, CB	O9, 6-ring	GLU 353 (A), LEU 387 (A)	H-donor, π–H	2.70, 4.05
3ERT – Trigonelline	O1, O1	NH2, NH2	ARG 394 (A), ARG 394 (A)	Ionic, Ionic	3.62, 3.56
1M17 – Diosgenin	OD1	O3	ASP 776 (A)	H-donor	2.95
1M17 – Quercetin	NZ, CB	O5, 6-ring	LYS 721 (A), PHE 699 (A)	H-acceptor, π–H	2.97, 4.38
1M17 – Trigonelline	NZ, NZ, NZ, NZ	O1, O1, O2, 6-ring	LYS 730 (A), LYS 851 (A), LYS 721 (A)	H-acceptor, Ionic, π–cation	2.94, 2.94, 3.15, 4.87
1GJH – Diosgenin	O	O3	ASP 35 (A)	H-donor	3.01
1GJH – Quercetin	OE2, NE	O9, O4	GLU 50 (A), ARG 6 (A)	H-donor, Ionic	2.92, 3.67
1GJH – Trigonelline	O, CA	C4, 6-ring	ALA 43 (A), GLY 46 (A)	H-donor, π–H	3.46, 3.87

3.10.4 Interaction Analysis

The types of interactions include hydrogen bonding, ionic interactions, and pi-stacking interactions, which play significant roles in determining the binding affinity. Diosgenin interacts with *ERα* ;3ERT, *EGFR*;1M17, and *Bcl-2*; 1GJH primarily through hydrogen bonds (H-donor), with distances ranging from 2.88 to 3.01 Å. These interactions suggest a stable binding configuration. Quercetin forms H-donor and pi-H interactions with *ERα, EGFR, and Bcl-2*, with distances varying from 2.70 to 4.38 Å. The pi-H interaction is especially notable for its potential in stabilizing the binding of Quercetin to EGFR. Trigonelline demonstrates both ionic and pi-cation interactions, especially with (*EGFR*; 1M17 and *Bcl-2* ;1GJH), where the ionic interactions involve residues such as LYS 730 and ARG 394, and pi-cation interactions are found with Lys residues. The docking results suggest that Diosgenin and Quercetin exhibit stronger binding affinities compared to Trigonelline, likely due to their ability to

form more stable interactions with the breast cancer-related proteins. Diosgenin's strong binding to *ERα* and Quercetin's strong binding to *Bcl-2* indicate their potential as effective inhibitors of these proteins. These compounds may play a crucial role in modulating estrogen receptor activity and inhibiting anti-apoptotic signaling pathways involved in cancer progression [28], Fig.18.

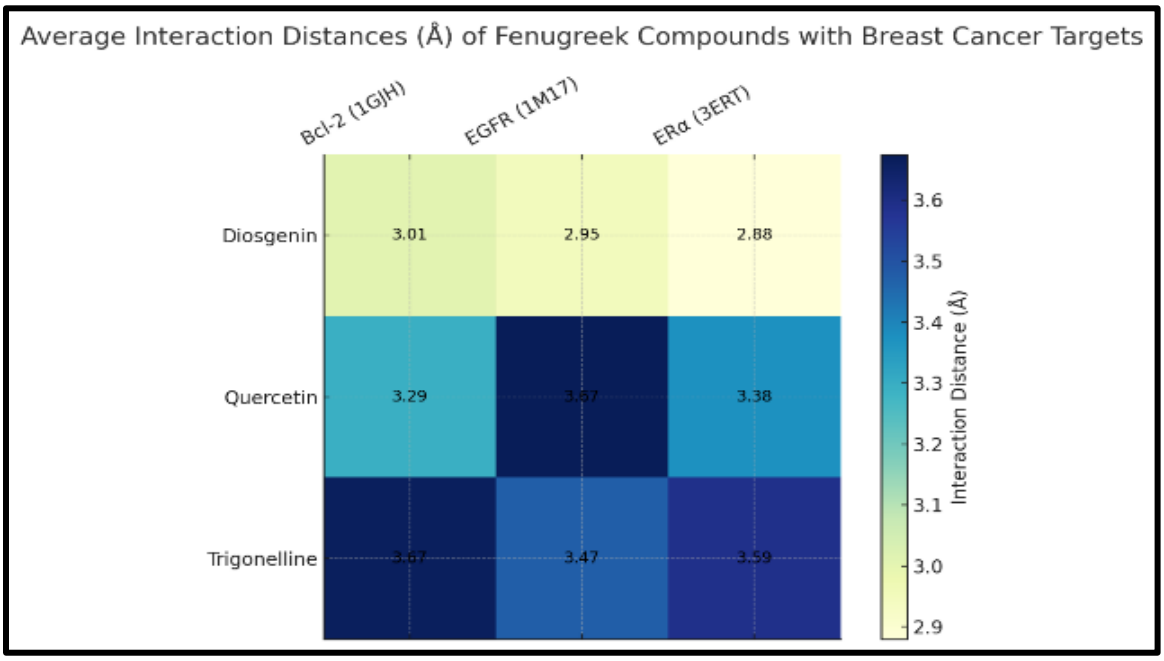

Fig (18): Heatmap of average interaction distance (A) between fenugreek-derived phytochemicals (Diosgnin, Quercetin, Trigonelline) and Breast cancer related protein targets (*ER alpha, EGFR, BCL-2*). Shorter distance (blue) indicates stronger and more stable ligand protein interactions

The present study demonstrated the successful green synthesis of silver nanoparticles (AgNPs) using aqueous fenugreek leaf extract and establishes their antioxidant, antimicrobial, and anticancer potential, complemented by molecular docking studies. The phytochemical analysis of fenugreek confirmed the presence of different compounds such as flavonoids , alkaloids , phenolics and saponins compounds known for their reducing and stabilizing ability during nanoparticle biosynthesis as well as for their biological activities[29] . This is consistent with previous reports that link fenugreek phytochemicals to antioxidant, anti-inflammatory, and anti-cancer properties[30]. The characteristic surface plasmon resonance(SPR) peak at 418nm which validated formation of AgNPs, aligning with earlier biogenic synthesis reports using other plant extracts[31] . FTIR analysis further confirmed the involvement of hydroxyl, carbonyl and amide groups in reduction and capping which indicating that proteins and phenolic compounds stabilized the NPs[32] . The emergence of Ag-O bonds at 513 strongly supports the formation of metallic silver. AFM imaging revealed size variations (62-80nm) depending on precursor concentration, highlighting the extract ability to control nanoparticle morphology. These results corroborate prior findings that plant extract act as both reducing and stabilize agents, yielding NPs with favorable physicochemical properties for biomedical use [33]. The aqueous fenugreek extract exhibited strong antioxidant activity in both DPPH and FRAP assays, surpassing vitamin C and Trolox at comparable concentration. This effect may be attributed to the high flavonoid and phenolic content, which enhance radical scavenging and electron donating capacity. when the oxidative given the stress pivotal role in carcinogenesis and microbial pathogenesis, these findings suggest that fenugreek derived NPs could provide dual benefits as antioxidative and as therapeutic agents [34]. The green synthesized AgNPs exhibits broad spectrum antimicrobial effect, with inhibition zones up to 33mm against *P.aeruginosa* and 42 mm against *Candida albicans*. These findings are in agreement with early reports demonstrating the efficacy of plant mediated AgNPs against both gram-positive and gram negative bacteria as well as fungi [35].The mechanism may involve AgNP binding to microbial cell walls, alteration of membrane permeability, and interaction with intracellular proteins and DNA , ultimately leading to cell death. The pronounced antifungal effect against *candida albicans further* expands the potential biomedical application of fenugreek mediated AgNPs, while the in-vitro assays revealed dose-dependent cytotoxicity of fenugreek mediated AgNPs.

toward MCF-7 cells, with an IC_{50} of 112.4, while sparing normal fibroblast (IC_{50}=140.4). This selectivity is critical for cancer therapeutics, reducing the likelihood of systemic toxicity. Similar studies have reported that AgNPs induce apoptosis through oxidative stress, mitochondrial dysfunction , and DNA damage [36].The results of present study support these mechanism and suggest that fenugreek NPs enhance cytotoxic potential while maintaining biocompatibility .when the molecular docking highlight diosgenin and quercetin as strong binders to breast cancer associated proteins, particular *ERα(*-9.2 kcal/mol) and BCL-2 (-9.1 kcal/mol). These results provide a mechanistic explanation for observed cytotoxicity in vitro, as inhibition of ER and *BCL-2* disrupt estrogen receptor signaling and anti-apoptotic pathways, respectively. While the trigonelline showed weaker interactions, but may still play supported role [37]. The combination of experimental cytotoxicity and computational docking strength the hypothesis that fenugreek derived phytochemicals synergize with AgNPs to exert anticancer effects. The present result suggests that fenugreek mediated AgNPs represent a promising multifunctional nanoplatform with potent antioxidant, antimicrobial and anticancer properties. Importantly, this study among the first studies, to integrate green synthesis, in vitro assays and in silico docking to provide a comprehensive understanding of fenugreek therapeutic potential in breast cancer. Nonetheless, further in vivo studies and pharmacokinetic evaluation are required to confirm efficacy and safety as well as to explore potential synergistic effects between AgNPs and fenugreek phytochemicals.

4- CONCLUSION

This study demonstrates that aqueous leaf extract of Trigonella *frenum-graecum* serves as an efficient and environmentally friendly bio reductant for the green synthesis of stable silver nanoparticles (AgNPs) with an average particle size of 62-80nm. The biosynthesized AgNPs exhibited a distinct surface Plasmon resonance at 418 nm, confirming successful nanoparticle formation and stabilization by phenolic and carbonyl functional groups. Functionally, fenugreek-mediated Ag-NPs showed strong antioxidant capacity, broad -spectrum antimicrobial activity, and selective cytotoxicity toward MCF-7 breast cancer cells (LC_{50}=112.4µg/mL) while sparing normal fibroblast (LC_{50}=140.4 µg/mL). These findings suggest that fenugreek-derived nanoparticles effectively combine biocompatibility with therapeutic potency. The complementary in silico docking analysis further revealed that major fenugreek phytochemicals-diosgenin and quercetin-bind strongly to apoptosis and proliferation related protein targets (*ERα*, *BCL-2*, *EGFR*) with binding energies ranging from -8.6 to -9.2 kcal/mol. Such interactions provide a plausible molecular mechanism underlying the observed in vitro anticancer effects through inhibition of estrogen receptor signaling and anti-apoptotic pathways. Overall, this integrative in vitro-in silico approach highlights fenugreek mediated AgNPs as a multifunctional biogenic Nano platform with promising antioxidant, antimicrobial, and anticancer potential. Future research should focus on in vivo efficacy, pharmacokinetic profiling, and mechanistic validation to further establish their value in breast cancer therapeutics.

REFERENCES

[1] Ahmad, F., Anwar, F., & Hira, S. J. (2016). Review on medicinal importance of Fabaceae family. *Journal Name*, *3*, 151–157.

[2] Nwozo, O. S., et al. (2023). Antioxidant, phytochemical, and therapeutic properties of medicinal plants: A review. *Journal Name*, *26*(1), 359–388. https://doi.org/10.1080/10942912.2022.2157425

[3] Leucuta, E. (2010). Nanotechnology for delivery of drugs and biomedical applications. *Current Clinical Pharmacology*, *5*(4), 257–280. https://doi.org/10.2174/157488410793352003

[4] Singh, H., et al. (2023). Revisiting the green synthesis of nanoparticles: Uncovering influences of plant extracts as reducing agents for enhanced synthesis efficiency and its biomedical applications. *International Journal of Nanomedicine*, 4727–4750. https://doi.org/10.2147/IJN.S419369

[5] Mikhailova, E. O. (2023). Selenium nanoparticles: Green synthesis and biomedical application. *Molecules*, *28*(24), 8125. https://doi.org/10.3390/molecules28248125

[6] Singla, P., & Dhillon, P. K. (2025). Characterization of bioactive compounds (BACs) in fenugreek. In *Fenugreek* (pp. 49–74). Apple Academic Press.

[7] Gao, J., et al. (2025). Rapid simultaneous determination of plant total flavonoids and polyphenols by merging zone flow injection spectrophotometry. *Analytical Methods*, *17*(33), 6719–6729. https://doi.org/10.1039/D5AY00994D

[8] Gulpinar, A. R., et al. (2012). Estimation of in vitro neuroprotective properties and quantification of rutin and fatty acids in buckwheat (*Fagopyrum esculentum* Moench) cultivated in Turkey. *Food Research International*, *46*(2), 536–543. https://doi.org/10.1016/j.foodres.2011.08.011

[9] Mboweni, H. F. (2018). *Antimicrobial, cytotoxic and preliminary phytochemical analysis of four medicinal plants and their formulation* (Unpublished thesis).

[10] Aylanc, V., et al. (2020). In vitro studies on different extracts of fenugreek (*Trigonella spruneriana* Boiss.): Phytochemical profile, antioxidant activity, and enzyme inhibition potential. *Journal of Food Biochemistry*, *44*(11), e13463. https://doi.org/10.1111/jfbc.13463

[11] Chung, K.-T., et al. (2025). Therapeutic potential of bioactive peptides derived from natural products of tortoiseshell and antler in alleviating osteoporosis and osteoarthritis. *International Journal of Molecular Sciences*, *26*(2), 581. https://doi.org/10.3390/ijms26020581

[12] Hazel, A., et al. (2025). Exploring the antioxidant potential and HPLC profile of fenugreek (*Trigonella foenum-graecum* L.) seed extracts. *NAJFNR*, *9*(19), 203–212. https://doi.org/10.51745/najfnr.9.19.203-212

[13] Gaona-Ruiz, M., et al. (2025). Covalent immobilization of the DPPH molecule in reusable smart polymers for the assessment of antioxidant capacity in beetroots. *Food Chemistry*, 146112. https://doi.org/10.1016/j.foodchem.2025.146112

[14] Qasim, H. S. (2024). The role of silver nanoparticles biosynthesized from *Citrus aurantium* leaves in vegetative and physiological characteristics of fenugreek plant (*Trigonella foenum-graecum* L.). *International Journal of Scientific Research and Applications*. https://doi.org/10.30574/ijsra.2024.11.2.0394

[15] Ansari, M., et al. (2023). Green synthesized silver nanoparticles: A novel approach for the enhanced growth and yield of tomato against early blight disease. *Microorganisms*, *11*(4), 886. https://doi.org/10.3390/microorganisms11040886

[16] Nishida, S., et al. (2008). Photothermal excitation and laser Doppler velocimetry of higher cantilever vibration modes for dynamic atomic force microscopy in liquid. *Review of Scientific Instruments*, *79*(12). https://doi.org/10.1063/1.3040500

[17] Aweda, F., Falaiye, O., & Oyewole, J. J. (2021). UV/VIS characterization and FT-IR analysis of harmattan dust across Sub-Sahara region of Africa. *Journal Name*, *14*(1). https://doi.org/10.47011/14.1.1

[18] Duan, M., et al. (2025). Enhancing subsurface imaging in ultrasonic atomic force microscopy with optimized contact force. *Ultramicroscopy*, *269*, 114094. https://doi.org/10.1016/j.ultramic.2024.114094

[19] U Din, M. M., et al. (2024). Green synthesis and characterization of biologically synthesized and antibiotic-conjugated silver nanoparticles followed by post-synthesis assessment for antibacterial and antioxidant applications. *ACS Omega*, *9*(17), 18909–18921. https://doi.org/10.1021/acsomega.3c08927

[20] Aziz, L., Hamza, S., & Abdul-Rahman, I. (2012). Isolation and characterization of phenazine produced from mutant *Pseudomonas aeruginosa*. *African Journal of Veterinary Sciences*, *5*, 42–53.

[21] Khorrami, S., et al. (2018). Selective cytotoxicity of green synthesized silver nanoparticles against the MCF-7 tumor cell line and their enhanced antioxidant and antimicrobial properties. *International Journal of Nanomedicine*, 8013–8024. https://doi.org/10.2147/IJN.S189295

[22] Almuzaini, N. A., et al. (2024). Mass spectrometric-based metabolomics of the Saudi cultivar of fenugreek (*Trigonella foenum-graecum* L.): A combined GC-MS, antimicrobial, and computational approach. *Pharmaceuticals*, *17*(12), 1733. https://doi.org/10.3390/ph17121733

[23] Haneen, D. S., et al. (2025). Synthesis, comprehensive in silico studies, and cytotoxicity evaluation of novel quinazolinone derivatives as potential anticancer agents. *Scientific Reports*, *15*(1), 23697. https://doi.org/10.1038/s41598-025-08062-7

[24] Kamel, M. D. (2025). Molecular and in silico analysis of pamidronate disodium interaction with type IV osteogenesis imperfecta caused by the ultra-rare COL1A1 variant rs72656337 (c.3664G>T; p.Ala1222Ser). *Genomics Reports*, 102367. https://doi.org/10.1016/j.genrep.2025.102367

[25] De Azevedo, D. Q., et al. (2024). A critical assessment of bioactive compounds databases. *Journal of Enzyme Inhibition and Medicinal Chemistry*, *16*(10), 1029–1051. https://doi.org/10.1080/17568919.2024.2342203

[26] Shrihastini, V., et al. (2021). Plant-derived bioactive compounds, their anti-cancer effects and in silico approaches as an alternative target treatment strategy for breast cancer: An updated overview. *Cancers*, *13*(24), 6222. https://doi.org/10.3390/cancers13246222

[27] Mbese, Z., Alven, S., & Aderibigbe, B. A. (2021). Collagen-based nanofibers for skin regeneration and wound dressing applications. *Polymers*, *13*(24), 4368. https://doi.org/10.3390/polym13244368

[28] Cao, S., et al. (2024). How hydrogen bonding and π–π interactions synergistically facilitate mephedrone adsorption by bio-sorbent: An in-depth microscopic scale interpretation. *Environmental Pollution*, *342*, 123044. https://doi.org/10.1016/j.envpol.2023.123044

[29] Pandey, P., et al. (2025). Biosynthesis of silver nanoparticles from plant extracts: A comprehensive review focused on anticancer therapy. *Frontiers in Pharmacology*, *16*, 1600347. https://doi.org/10.3389/fphar.2025.1600347

[30] Nallappan, D., et al. (2021). Green biosynthesis, antioxidant, antibacterial, and anticancer activities of silver nanoparticles of *Luffa acutangula* leaf extract. *BioMed Research International*, *2021*(1), 5125681. https://doi.org/10.1155/2021/5125681

[31] Mohammed, R., et al. (2024). The importance of using fenugreek (Trigonella foenum-graecum L.) in broiler feeds: A review. Journal Name, 4(4). https://doi.org/10.56286/wd7wyd36

[32] Saha, N., Trivedi, P., & Dutta Gupta, S. J. (2016). Surface plasmon resonance (SPR)-based optimization of biosynthesis of silver nanoparticles from rhizome extract of Curculigo orchioides Gaertn. and its antioxidant potential. Journal of Cluster Science, 27(6), 1893–1912.

[33] Yadav, S., et al. (2024). Biogenic synthesis of nanomaterials: Bioactive compounds as reducing and capping agents. In Biogenic nanomaterials for environmental sustainability: Principles, practices, and opportunities (pp. 147–188). Springer. https://doi.org/10.1007/978-3-031-45956-6_6

[34] Villagrán, Z., et al. (2024). Plant-based extracts as reducing, capping, and stabilizing agents for the green synthesis of inorganic nanoparticles. Resources, 13(6), 70. https://doi.org/10.3390/resources13060070

[35] Faisal, Z., et al. (2024). The multifaceted potential of fenugreek seeds: From health benefits to food and nanotechnology applications. Food Science & Nutrition, 12(4), 2294–2310. https://doi.org/10.1002/fsn3.3959

[36] Mustafa, D.A. (2025). Prevalence of Risk Factors for Breast Tumors Detected by Mammography a Cross-Sectional Study. Dijlah Journal of Medical Sciences, 2(1): 72-81.

[37] Ahmad, R., et al. (2025). Exploring the role of phytochemical classes in the biological activities of fenugreek (Trigonella foenum-graecum): A comprehensive analysis based on statistical evaluation. Foods, 14(6), 933. https://doi.org/10.3390/foods14060933